

Precipitation estimations based on remote sensing compared with data from weather stations over agricultural region of Argentina pampas

Gustavo Ovando^a, Silvina Sayago^a, Yanina Bellini^b, María Laura Belmonte^b, Mónica Bocco^{a,*}

^a Facultad de Ciencias Agropecuarias, Universidad Nacional de Córdoba. Córdoba, Argentina

^b Estación Experimental Anguil "Ing. Agr. Guillermo Covas" - INTA. Anguil, La Pampa, Argentina



ARTICLE INFO

Keywords:

Rainfall
IMERG
Taylor diagram
Buenos Aires
Córdoba
La Pampa
Santa Fe

ABSTRACT

Global patterns of precipitation have changed due to the increase in temperature as a result of climate change. Measuring the amount of precipitation at a given location using surface instruments is relatively simple. However, the great spatial and temporal variability of the intensity, type and occurrence of this phenomenon, makes direct and uniformly calibrated measurements difficult in large regions. Satellite information is an important alternative to describe precipitation events; the Global Precipitation Measurement (GPM) mission estimates precipitation, considering different time periods, with three products Integrated Multi-Satellite Retrievals for GPM (IMERG), in near real time. This study evaluates and quantifies, temporally and spatially, the monthly precipitation estimated by Early (IMERG-E), Late (IMERG-L) and Final (IMERG-F) products compared with data from weather stations located in agricultural areas of the Pampas region in Argentina. Data of precipitation belonging to meteorological stations located at four provinces: Buenos Aires, Córdoba, La Pampa and Santa Fe, for 2014–2018 periods, were considered. The spatial performance of IMERG was evaluated using statistical coefficients and Taylor diagrams, considering at region, province and stations level. The adjustment of the products increased from IMERG-E to IMERG-F, obtaining R^2 values between 0.86 and 0.95 and RMSE from 14.2 to 29.3 mm, the best results corresponding to Córdoba and the worst to La Pampa. The performance of GPM products varies temporally; IMERG-F presented a higher correlation coefficient and a lower percent root mean square error in warm than in cold seasons. The results indicate that GPM can effectively capture the amount and patterns of monthly precipitation over the Pampas region of Argentina, which is important for its application to agricultural production and disaster prevention.

1. Introduction

Worldwide availability of water is based mainly on rainfall and oceans reserves. Global patterns of precipitation have changed due to the increase in temperature as a result of climate change. Therefore, the demand for fresh water and its reserves are affected at local, regional and global scales (Bano and Arshad, 2018). Extreme rainfall events associated with floods, droughts and landslides have important socio-economic impacts. On the other hand, the administration of water resources, whether for irrigation, agriculture, flood control, drought or freshwater management, requires accurate and timely knowledge of when, where and how much it rains (Hou et al., 2014).

Measuring the amount of precipitation at a given location using surface instruments is relatively simple. However, the great spatial and temporal variability of the intensity, type and occurrence of this

phenomenon, makes direct and uniformly calibrated measurements difficult in large regions. On the surface, rain gauges also present problems of representativeness when estimating rainfall in large areas, or in short periods of time (Hou et al., 2014; Boluwade et al., 2017) or in regions with sparse meteorological networks, as it is common to find in mountainous terrain and/or developing countries (Ulloa et al., 2017).

The Argentine Pampas is the main agricultural region of Argentina, occupying a surface of 613.500 km² (Aliaga et al., 2017); its economy is based on agriculture with soybean (*Glycine max L. Merr.*), corn (*Zea mays L.*), wheat (*Triticum spp.*) and sunflower (*Helianthus annuus L.*) as dominant crops (Nolasco et al., 2021). In spite of its relevance, crop production in this zone remains highly dependent on precipitation as irrigation is still marginal, less than 1% on an area basis for sprinkler irrigation (Veron et al., 2015). However this area has a sparse and irregularly distributed weather station network, which does not

* Corresponding author.

E-mail addresses: mbocco@gmail.com, mbocco@gmail.com (M. Bocco).

adequately reflect the characteristic of rainfall spatial variability.

Several studies indicate that the westward advance of the agricultural frontier in the Pampas region during the last quarter of the twentieth century was favored by an increase in rainfall; the region experiences abrupt changes in its precipitation regime, which cause severe impacts in its agricultural economy and its environmental stability. This situation creates the risk that the agricultural production system may exceed the environment's carrying capacity, leading to decreased production and environmental degradation (Pérez et al., 2015). For this reason, it is important for producers and decision-makers in agricultural policies to have a tool that allows obtaining accurate and real-time regional rainfall estimates.

In this context, satellite information is an important alternative to describe precipitation events at different spatio-temporal scales. In the last decades, the advance in technology allowed the development of a series of global precipitation products, derived from satellites (Chen and Li, 2016) covering long periods of time and large areas (Ovando et al., 2018). These products are based on calibrated infrared and microwave observations from different satellite missions, using a variety of fusion techniques. While infrared sensors on geostationary satellites can provide precipitation estimates at high temporal resolutions, microwave sensors (on polar orbiting satellites) remain the instrument of choice for estimating precipitation, since radiative signatures are more directly related to precipitating particles (Hou et al., 2014).

An example of the infrared observations with passive microwaves combination is the Tropical Rainfall Measuring Mission (TRMM) product; it was the first satellite mission dedicated to observing and understanding tropical and subtropical rainfall, which stopped operating in 2015. One of the main limitations of TRMM is that it did not adequately estimate solid precipitation or low intensity rainfall (<0.5 mm/h), and its sampling frequency was from 15 h to 4 days, which introduced errors in the estimates. Another restriction of TRMM was the lack of coverage at high latitudes (>37° N/S). The Global Precipitation Measurement (GPM) mission was developed to overcome these problems, covering the region between 65°S and 65°N, with a temporal resolution of 3 h and including solid and little intense precipitation (Boluwade, 2020).

The products generated by Integrated Multi-Satellite Retrievals for GPM (IMERG) are available in near real time: IMERG-E (IMERG Early) and IMERG-L (IMERG Late), and with greater delay, IMERG-F (IMERG Final), because it is compared with the monthly rain gauge information. IMERG-E images are produced for users who need a quick response related to warnings for flood or landslide potentials; instead IMERG-L is aimed at users working on agricultural forecasting or drought monitoring. IMERG-F estimates are the most accurate and reliable and are used for research (Sungmin et al., 2017; Huang et al., 2018).

The objective of this study was to quantitatively evaluate, temporally and spatially, the monthly precipitation estimated by Early, Late and Final GPM products compared with data from weather stations located

in agricultural areas of the Pampas region in Argentina.

2. Material and methods

2.1. Study area and meteorological data

The Argentine Pampas is a wide and fertile plain that includes Buenos Aires, La Pampa, Córdoba and Santa Fe provinces (Fig. 1). Total area in these four provinces is approximately 614,000 km². This region is characterized by the occurrence of long periods of drought and floods, which affect the water availability, the productivity of agricultural systems and other human activities (Aliaga et al., 2017).

The Pampas has, mainly, a humid temperate climate. Rains are generated by latitudinal and longitudinal movements of air masses. Annual rainfall decreases from northeast to southwest and determines the passage from warm and humid climate to a semi-arid one; this region is under the influence of the South Atlantic high-pressure and it represents the subtropical area of Argentina. The dry westerly winds predominate at the southern extreme of the region. (Pérez et al., 2015; Aliaga et al., 2017). El Niño Southern Oscillation (ENSO) causes inter-annual rainfall variations with more intensity during autumns and summers (Grimm, 2011).

Daily precipitation registers for 45 selected weather stations were supplied by Servicio Meteorológico Nacional (SMN) and Instituto Nacional de Tecnología Agropecuaria (INTA). These stations are located in Buenos Aires (Table 1), Córdoba (Table 2), La Pampa (Table 3) and Santa Fe (Table 4) provinces and they are representative of the

Table 1

Geographical location and missing percentage of registered precipitation data for Buenos Aires stations used in this study (March 2014–June 2018).

Station ID	Station	Latitude (°)	Longitude (°)	Elevation (masl)	Missing Data (%)
1	Adolfo G. Chaves	-37.93	-60.05	214	0.0
2	Balcarce	-37.76	-58.30	134	0.0
3	Chascomús	-35.75	-58.01	16	34.6
4	Cnel.	-38.83	-61.23	58	0.0
	Dorrego				
5	De La Garma	-38.06	-60.46	174	0.0
6	Lincoln	-34.85	-61.52	76	17.3
7	Ochandio	-38.37	-59.91	107	0.0
8	Pergamino	-33.93	-60.55	61	1.9
9	Rauch	-36.77	-59.10	87	17.3
10	San Pedro	-33.77	-59.75	37	1.9
11	Trenque Lauquen	-35.96	-62.73	80	1.9
12	Tres Arroyos	-38.21	-60.32	143	1.9
13	25 de Mayo	-35.42	-60.17	58	0.0

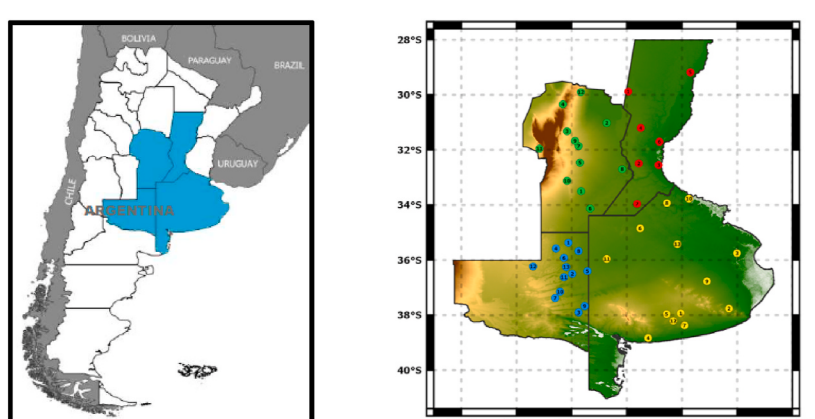


Fig. 1. Geographical location of Pampas region in Argentina, and meteorological stations considered in this study.

Table 2

Geographical location and missing percentage of registered precipitation data for Córdoba stations used in this study (March 2014–June 2018).

Station ID	Station	Latitude (°)	Longitude (°)	Elevation (masl)	Missing Data (%)
1	Alejandro Roca	-33.50	-63.66	180	1.9
2	Balnearia	-31.02	-62.73	89	5.8
3	Córdoba	-31.32	-64.17	474	0.0
4	Dean Funes	-30.34	-64.32	688	1.9
5	Hernando	-32.46	-63.70	268	5.8
6	Laboulaye	-34.13	-63.33	137	0.0
7	Manfredi	-31.86	-63.75	296	1.9
8	Marcos Juarez	-32.70	-62.17	114	0.0
9	Pilar	-31.67	-63.88	338	0.0
10	Río Cuarto	-33.12	-64.17	420	0.0
11	Villa Dolores	-31.95	-65.17	569	0.0
12	Villa de María del Río Seco	-29.90	-63.67	341	0.0

Table 3

Geographical location and missing percentage of registered precipitation data for La Pampa stations used in this study (March 2014–June 2018).

Station ID	Station	Latitude (°)	Longitude (°)	Elevation (masl)	Missing Data (%)
1	Alta Italia	-35.37	-64.12	163	11.5
2	Anguil	-36.50	-63.98	156	3.8
3	Bernasconi	-37.90	-63.75	163	5.8
4	Caleufú	-35.58	-64.57	204	19.2
5	Catriló	-36.40	-63.43	127	9.6
6	Eduardo Castex	-35.92	-64.28	190	3.8
7	Gral. Acha	-37.38	-64.60	238	5.8
8	Gral. Pico	-35.67	-63.75	139	1.9
9	Guatrache	-37.67	-63.53	174	9.6
10	Quehué	-37.15	-64.42	232	3.8
11	Santa Rosa	-36.62	-64.28	183	1.9
12	Victorica	-36.23	-65.40	309	3.8
13	Winifreda	-36.25	-64.20	152	7.7

Table 4

Geographical location and missing percentage of registered precipitation data for Santa Fe stations used in this study (March 2014–June 2018).

Station Number	Station	Latitude (°)	Longitude (°)	Elevation (masl)	Missing Data (%)
1	Ceres	-29.88	-61.95	87	0.0
2	Las Rosas	-32.49	-61.57	98	3.8
3	Oliveros	-32.55	-60.85	21	0.0
4	Rafaela	-31.20	-61.50	100	5.8
5	Reconquista	-29.18	-59.70	48	0.0
6	Sauce Viejo	-31.70	-60.82	17	0.0
7	Villa Cañas	-33.96	-61.63	102	3.8

agroclimatic conditions for the different agricultural systems of Argentine Pampas. The precipitation data were obtained from March 2014 to July 2018 and they were accumulated in monthly values.

Fig. 1 shows the weather stations considered in this study, which cover Buenos Aires, Córdoba, La Pampa and Santa Fe provinces.

2.2. GPM data

The GPM mission estimates precipitation by using a combination of passive microwave and infrared satellites comprising the GPM constellation. IMERG version 5 (V05) level 3 products were used in this study. The level 3 products include gridded rainfall and snowfall data, with $0.1^\circ \times 0.1^\circ$ spatial resolution and 30 min temporal resolution. GPM daily data used in this work were obtained online from Giovanni ([ps://giovanni.gsfc.nasa.gov/](http://giovanni.gsfc.nasa.gov/)) available at three different processing levels, in near-real time with 6 h, 18 h, and 2-month latencies. These latencies are called early, late, and final runs, respectively. IMERG-E and IMERG-L runs are calibrated with climatological coefficients that vary month by month, as well as by location. On the other hand, IMERG-F run is calibrated and adjusted using monthly gauge data from weather stations (Sungmin et al., 2017).

The IMERG information of the three processing levels corresponding to the pixel of each meteorological station was acquired and they were accumulated in monthly values. In Fig. 2 an output sample of GPM product (IMERG-F) from 2014 to 2018 period, can be observed.

2.3. Metrics for accuracy assessment

The accuracy of monthly precipitation values provided by GMP with those recorded at meteorological stations was evaluated with coefficient of determination (R^2), root mean square error ($RMSE$) and percent root mean square error (% $RMSE$).

In order to facilitate the stations inter-comparison, we present a Taylor diagram (Taylor, 2001). This graph shows the standard deviation (SD), correlation coefficient (r), and the centered root mean square error (RMSEc) values normalized by the reference SD, which is defined as:

$$RMSEc = n^{-1} \sqrt{\sum_{i=1}^n \left[\left(\frac{P_{GPM} - \bar{P}_{GPM}}{P_{GPM}} \right)^2 - \left(\frac{P_{reg} - \bar{P}_{reg}}{P_{reg}} \right)^2 \right]} / n^{-1} \sum_{i=1}^n P_{reg}$$

where n is the number of observations, P_{reg} is the in situ registered precipitation and \bar{P}_{reg} is its average. P_{GPM} and \bar{P}_{GPM} are, respectively, the precipitation and its average estimated by GPM, for all considered periods.

3. Results and discussion

For the Argentine Pampas region, Fig. 3 shows maximum (A) and minimum (B) monthly precipitation values registered from March 2014 to June 2018. For monthly maximum precipitation, the stations with higher values are concentrated towards the west; although, the highest value for the whole period was registered in Reconquista (Santa Fe). Monthly minimum precipitation has a more uniform spatial distribution than the maximum values. In most stations the monthly minimum registered values are below 3 mm and the four provinces present, at least, one station with monthly minimum registered precipitation value greater than or equal to 5 mm.

The values of maximum and minimum precipitation registered and informed by GPM, for each station, considering the analyzed period (March 2014–June 2018), are presented, for all provinces, in Tables 5–8.

When the maximum monthly precipitation is analyzed, it is observed that in all stations of Buenos Aires province (Table 5) the values oscillate between 160 and 250 mm, except for Pergamino and Rauch, which registered 295 mm and 61 mm, respectively. These extreme values are also informed by GPM data, with maximum monthly precipitation values between 271 and 405 mm/254 and 373 mm/157 and 275 mm for IMERG-E/IMERG-L/IMERG-F, respectively.

The best adjustment can be observed for Cordoba province (Table 6), where the maximum registers were between 180 and 360 mm; this data range is similar to records reported by IMERG-E, IMERG-L and IMERG-F (from 155 to 397 mm).

The values recorded in La Pampa (Table 7) are from 200 to 400 mm. Maximum precipitation is on the order of those reported by IMERG-F, while they are widely exceeded by IMERG-E and IMERG-L. These last two products reported for Quehué a maximum value greater than 600 mm per month, while 322 mm were registered.

Santa Fe province (Table 8) presented the highest monthly

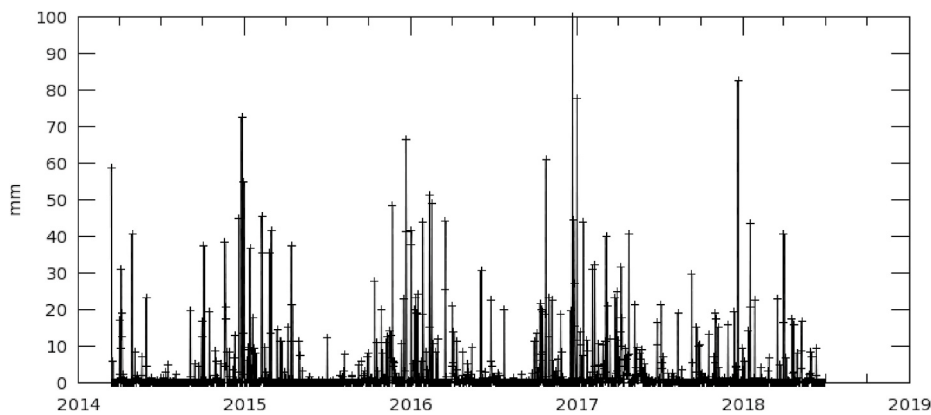


Fig. 2. Time series of daily accumulated precipitation from GPM IMERG-F v05 product, corresponding to Laboulaye station (March 2014 to June 2018).

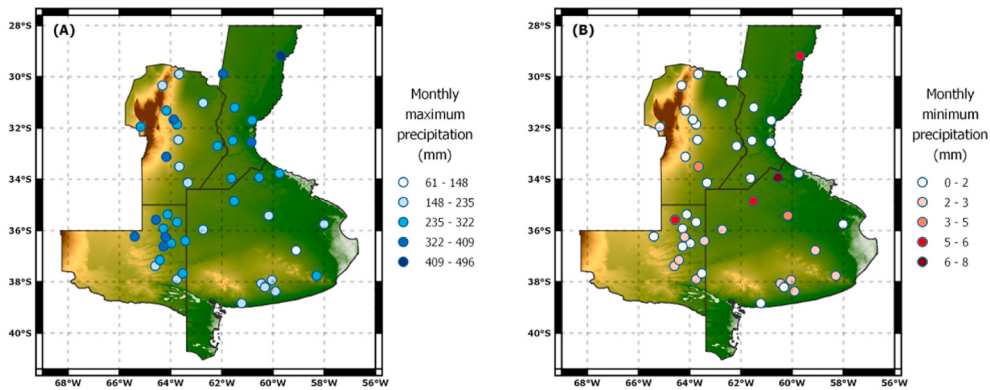


Fig. 3. Monthly maximum (A) and minimum (B) precipitation registered values, from March 2014 to June 2018, for each station considered in this study.

Table 5

Monthly maximum and minimum values of registered precipitation and GPM data, in mm, for Buenos Aires stations (March 2014–June 2018).

Station ID	Station	Registered max/min	IMERG-E max/min	IMERG-L max/min	IMERG-F max/min
1	Adolfo G. Chaves	163/2	284/11	254/12	157/4
2	Balcarce	249/3	334/11	311/9	220/3
3	Chascomús	206/0	330/11	305/7	234/12
4	Cnel. Dorrego	206/1	392/6	377/4	244/3
5	De La Garma	217/3	271/9	264/7	182/4
6	Lincoln	273/5	309/4	356/3	246/3
7	Ochandío	162/3	268/6	288/5	189/3
8	Pergamino	295/8	356/10	314/11	256/10
9	Rauch	61/3	47/12	40/12	45/5
10	San Pedro	245/0	310/5	274/2	275/8
11	Trenque Lauquen	199/3	295/3	270/2	225/2
12	Tres Arroyos	211/1	299/6	318/5	208/4
13	25 de Mayo	204/4	405/4	373/1	220/4

precipitation records informed for its stations and IMERG products, throughout the whole Pampas region. Particularly, in Reconquista, 496 mm were registered and GPM estimated between 480 and 564 mm.

For the whole study region, in most of the stations there were months where no rainfall occurred; the highest record of minimum precipitation, of 8 mm, was registered in Pergamino (Buenos Aires).

Fig. 4 shows monthly precipitation estimates derived from IMERG-E, IMERG-L and IMERG-F products against registered measurements over

Table 6

Monthly maximum and minimum values of registered precipitation and GPM data, in mm, for Córdoba stations (March 2014–June 2018).

Station ID	Station	Registered max/min	IMERG-E max/min	IMERG-L max/min	IMERG-F max/min
1	Alejandro Roca	225/4	257/4	225/5	228/4
2	Balnearia	187/1	170/0	156/0	210/0
3	Córdoba	317/0	298/0	273/0	349/0
4	Dean Funes	182/0	205/0	189/0	154/0
5	Hernando	204/1	256/1	244/1	255/0
6	Laboulaye	231/0	274/0	280/0	247/0
7	Manfredi	281/0	338/0	258/0	317/0
8	Marcos	286/0	305/1	262/1	301/1
9	Juarez				
10	Pilar	352/0	289/0	329/0	397/0
11	Río Cuarto	358/0	372/1	326/1	360/1
12	Villa Dolores	247/0	260/0	264/0	246/0
	Villa de María del Río Seco	176/0	185/0	187/0	184/0

the entire Pampas region. The IMERG-F product presents the best performance, with $R^2 = 0.91$ and RMSE = 20.4 mm; for IMERG-E/IMERG-L products these statistics are equal to 0.69/0.70 and 55.6/53.4 mm, respectively. Note that these last two products show overestimation with respect to monthly registered precipitation, which is observed by the positive difference between regression line (red line in Fig. 4) and identity line (1:1 dotted black line in Fig. 4). Part of the errors observed may be due to a considerable representativeness error because of point-to-area comparison and differences in precipitation measuring principles from the pluviometers and satellites (Prakash et al., 2017). These

Table 7

Monthly maximum and minimum values of registered precipitation and GPM data, in mm, for La Pampa stations (March 2014–June 2018).

Station ID	Station	Registered max/min	IMERG-E max/min	IMERG-L max/min	IMERG-F max/min
1	Alta Italia	260/0	350/1	379/0	275/1
2	Anguil	262/0	337/2	301/2	287/2
3	Bernasconi	191/3	514/10	439/13	223/9
4	Caleufú	399/5	510/15	474/18	325/14
5	Catriló	257/2	301/17	307/7	266/7
6	Eduardo Castex	291/0	426/1	476/0	301/1
7	Gral. Acha	214/2	342/15	378/11	229/1
8	Gral. Pico	259/0	429/1	490/0	276/0
9	Guatrache	238/1	498/3	453/2	227/4
10	Quehué	322/2	608/10	636/8	354/5
11	Santa Rosa	326/0	522/1	587/2	321/1
12	Victorica	330/0	348/0	375/0	312/0
13	Winifreda	378/3	463/4	505/6	307/5

Table 8

Monthly maximum and minimum values of registered precipitation and GPM data, in mm, for Santa Fe stations (March 2014–June 2018).

Station Number	Station	Registered max/min	IMERG-E max/min	IMERG-L max/min	IMERG-F max/min
1	Ceres	342/0	298/0	263/0	290/0
2	Las Rosas	290/1	334/5	411/6	261/5
3	Oliveros	356/0	336/1	335/6	308/3
4	Rafaela	282/0	313/1	278/1	252/2
5	Reconquista	496/5	564/2	519/5	480/6
6	Sauce Viejo	266/0	267/4	277/7	280/3
7	Villa Cañas	258/1	334/5	411/6	261/5

first results suggest that the IMERG-F product has great application potential for water resources planning and management, however we must take into account the disadvantage of its high latency.

Earlier studies have also shown that the performance of IMERG in other regions was similar to our results. [Tan and Santo \(2018\)](#) reported RMSE values of 118.37, 114.33 and 97.01 mm/month for IMERG-E, IMERG-L and IMERG-F, respectively, when comparing these products with 501 precipitation gauges distributed across Malaysia from March 2014 to February 2016. [Chen and Li \(2016\)](#), for sub-regions of Mainland China, obtained R^2 from 0.62 to 0.92 and RMSE of 178.5 mm, estimating annual precipitation from the IMERG-F product.

In order to determine the differences in the capability of IMERG to show the precipitation in each province of the Pampas region, we examined the scatter-plot between registered and GPM informed one.

[Fig. 5](#) shows, for all stations localized in each province, the satellite-

derived precipitation plotted against registered measurements. When IMERG-E and IMERG-L products are compared, minor differences in performance are observed between them. In La Pampa and Buenos Aires provinces there are overestimations of monthly precipitation, while in Córdoba and Santa Fe no over/underestimation patterns are detected. These products, for Buenos Aires, La Pampa and Santa Fe, have R^2 values from 0.63 to 0.77 and RMSE between 51.7 and 58.0 mm. In Córdoba province, a better performance of these products is observed, with R^2 and RMSE values near to 0.81 and 30.0 mm, respectively.

The IMERG-F product strongly improves the adjustments with the registered values, increasing the R^2 values (between 0.86 and 0.95) and decreasing the RMSE to almost half (from 14.2 to 29.3 mm). The best results belong to Córdoba, which could be explained by a better control of surface observations.

Based on the previous results, as the IMERG-F product shows the best performance for Pampas region and each province, we will only analyze this product from here on. [Tan and Santo \(2018\)](#) also reported that the IMERG-F product provides more accurate precipitation information compared to the near real-time products.

[Fig. 6](#) shows a Taylor diagram based on the r , SD and RMSEc statistics, for each Pampas province. This diagram provides a way of graphically summarizing how closely a set of patterns matches observations. Each point in the two-dimensional Taylor diagram represents, simultaneously, the three statistics for each station ([Taylor, 2001](#)).

Taylor diagram ([Fig. 6](#)) shows that the stations of Córdoba province are, in relative position, closer to the reference dot than the rest of the provinces (with the exception of Hernando). Inversely, the stations in Santa Fe show a dispersed distribution when the three adjustment statistics are considered, highlighting an overall lower ability of GPM to correctly represent monthly precipitation in this province.

Considering the stations located in Buenos Aires and La Pampa, we observe that the statistics included in Taylor diagram achieve close values, although their distribution changes its format when the correlation coefficients (Buenos Aires) or the standard deviations (La Pampa) are calculated. Using Taylor diagrams, [Tang et al. \(2016\)](#) indicated that IMERG data are closer to observations than the other satellite products, indicating that GPM is reliable for estimating rainfall.

The main crops in Pampas region are soybean and corn (with growth period in spring and summer) and wheat (winter period principally); for this reason, it is important to compare the performance of precipitation estimates from IMERG, considering two seasons: warm and cold. [Verón et al. \(2015\)](#) affirm that despite its relevance, crop production in the Pampas remains highly dependent on precipitations as irrigation is still marginal (less than 1 % on an area basis for sprinkler irrigation). On the other hand, methodologies for evaluating the impact of climate on crop yields include working with crop simulation models, and these require precipitation among their input data.

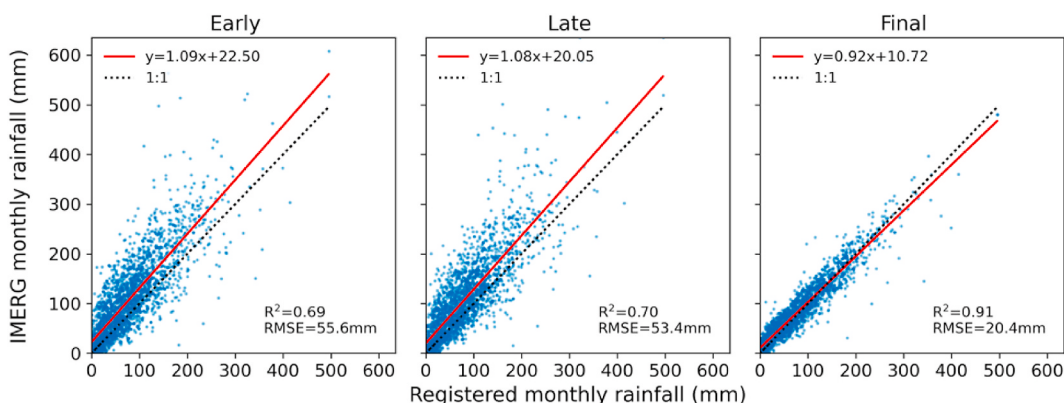


[Fig. 4](#). Scatter plots of registered versus IMERG-E, IMERG-L and IMERG-F monthly precipitation for the whole Pampas region (March 2014–June 2018). The regression and identity (1:1) lines are represented by red and black dotted ones, respectively. (For interpretation of the references to colour in this figure legend, the reader is referred to the Web version of this article.)

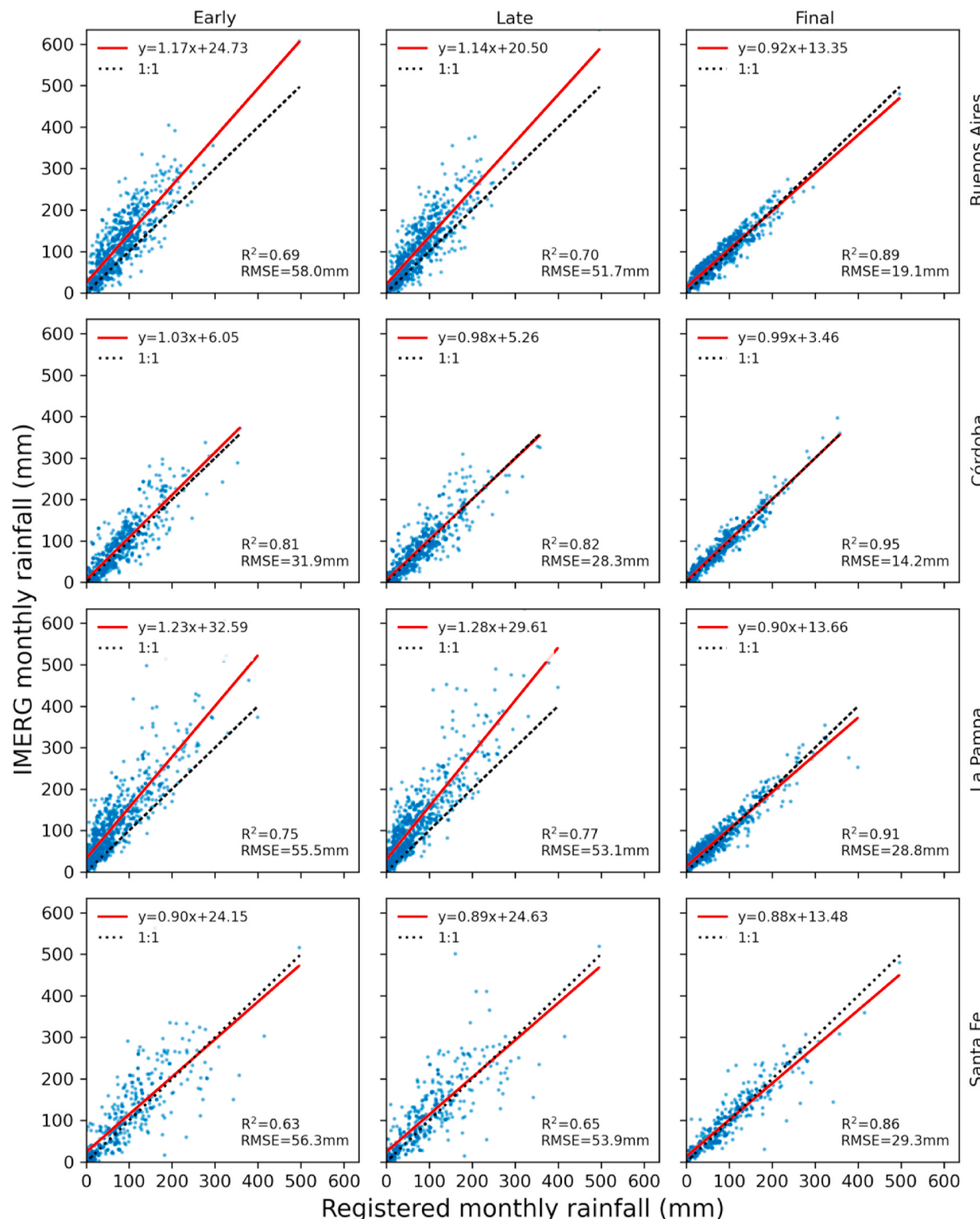


Fig. 5. Scatter plots of registered versus IMERG-E, IMERG-L and IMERG-F monthly precipitation for Buenos Aires, Córdoba, La Pampa and Santa Fe provinces (March 2014–June 2018). The regression and identity (1:1) lines are represented by red and black dotted ones, respectively. (For interpretation of the references to colour in this figure legend, the reader is referred to the Web version of this article.)

Fig. 7 shows correlation coefficients and %RMSE values, obtained from the adjustment between IMERG-F and precipitation data registered, considering warm season (spring and summer) and cold season (autumn and winter).

Fig. 7 allows us to affirm that IMERG-F presents a greater adjustment in most of the stations of the region in the warm season. This behavior was also reported by Wang et al. (2019), who evaluated IMERG products

on a seasonal scale and reported a better performance in warm than in cold seasons. These results are encouraging for the forecast of rainfall in the growth period of soybean and corn.

For all provinces considered in this study, the data fit does not present a homogeneous spatial pattern. In warm season, %RMSE values are between 9.5 % and 33.4 %, while in the cold season they are from 15.6 % to 49.2 %, with the exception of Ceres and Rafaela stations, which

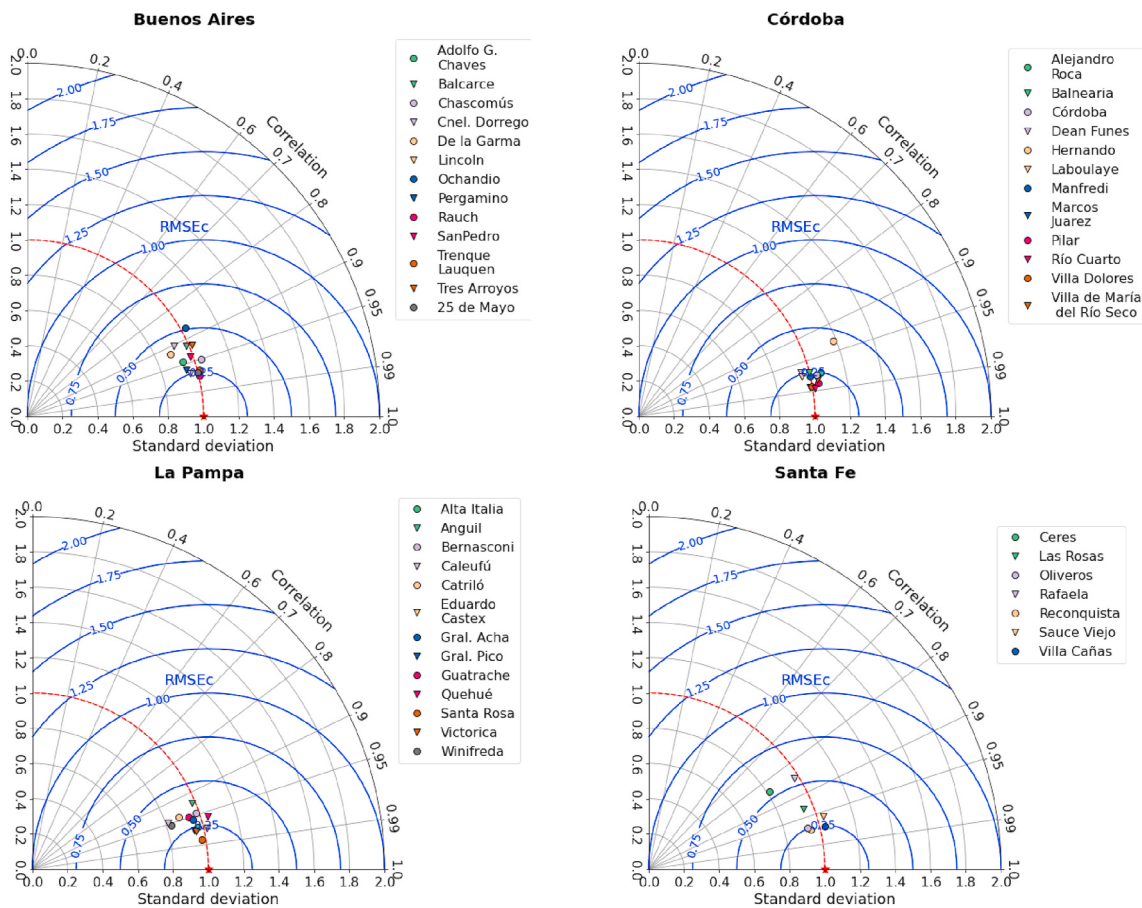


Fig. 6. Taylor diagrams based on the correlation coefficient (r), standard deviation (SD), and centered root mean square error (RMSEc) of registered measurements versus monthly precipitation estimates derived from IMERG-F product, for Buenos Aires, Córdoba, La Pampa and Santa Fe provinces. The red star symbol represents the reference dot. (For interpretation of the references to colour in this figure legend, the reader is referred to the Web version of this article.)

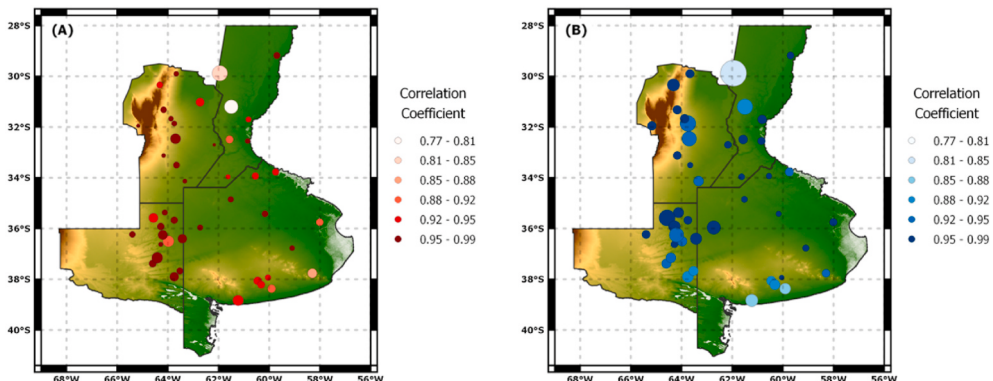


Fig. 7. Correlation coefficient and percent root mean square error of monthly precipitation registered measurements versus monthly precipitation estimates derived from IMERG-F for warm (A) and cold (B) season, for all stations in Pampas region (circle with the smallest diameter indicates %RMSE = 9 % and the one with the largest diameter %RSME = 79.7 %).

present a %RMSE of 46.4%/79.7 % and 42.2 %/47.7 % for warm/cold season, respectively. The lowest values of correlation coefficients occur in Santa Fe province, with $r = 0.77$ (Rafaela) for warm season and $r = 0.83$ (Ceres) for cold season, and the largest obtained value is $r = 0.99$, for both seasons, in Córdoba and La Pampa.

Salles et al. (2019) showed that GPM data present a strong seasonal variability; they affirm that IMERG-F performed better during the wet season than during the dry season. This problem in the seasonally adjustment is also reported by Sun et al. (2018). Chen and Li (2016) observed, over Mainland China, that IMERG estimation varies greatly

spatially and temporally, and they showed worse performance in winter.

4. Conclusions

In this study early, late and final GPM monthly precipitation products were evaluated and compared with data from 45 weather stations located in four provinces of Pampas region (Argentina), during the period from March 2014 to June 2018.

The three IMERG products performed well estimating the monthly precipitation registered, considering the Pampas region as a whole;

although the final product IMERG-F is the most accurate. The IMERG-E and IMERG-L products presented very good statistical values for the region; they were also evaluated because the longer latency of IMERG-F makes it unsuitable for near-real-time applications.

The IMERG-F product, when each province was considered separately, improved the fit from La Pampa, Santa Fe, Buenos Aires to Córdoba. The statistical analysis from the Taylor diagram allowed identifying, in each province, the stations where the use of the IMERG-F product would be more reliable.

The performance of IMERG-F varies temporally, observing a higher correlation coefficient in warm than in cold seasons. This indicates GPM can effectively capture the seasonal patterns of precipitation over the Argentine Pampas region, which is important to summer crops management.

We propose in the future, as a continuity of this line of work, to evaluate various factors such as elevation, topography, and longitudinal and latitudinal gradient and adjustment when daily time periods or accumulated abundant precipitation are considered. In the Pampas Region, GPM products are important for its application to agricultural production and disaster prevention.

Ethical statement

We are submitting the manuscript “**Precipitation estimations based on remote sensing compared with data from weather stations over agricultural region of Argentina Pampas**” to **Remote Sensing Applications: Society and Environment**. All ethical practices have been followed in relation to the development, writing, and publication of this article.

CRediT authorship contribution statement

Gustavo Ovando: Conceptualization, Methodology, Software, Resources, Formal analysis, Validation, Writing – original draft, Writing – review & editing. **Silvina Sayago:** Conceptualization, Methodology, Data curation, Formal analysis, Resources, Validation, Writing – original draft, Writing – review & editing. **Yanina Bellini:** Writing – original draft, Resources. **María Laura Belmonte:** Writing – original draft, Resources. **Mónica Bocco:** Project administration, Conceptualization, Methodology, Data curation, Formal analysis, Resources, Validation, Investigation, Writing – original draft, Writing – review & editing.

Declaration of competing interest

The authors declare that they have no known competing financial interests or personal relationships that could have appeared to influence the work reported in this paper.

Acknowledgements

This work was partially supported by Secretaría de Ciencia y Técnica (SECYT)–Universidad Nacional de Córdoba, Argentina.

References

- Aliaga, V.S., Ferrelli, F., Piccolo, M.C., 2017. Regionalization of climate over the Argentine Pampas. *Int. J. Climatol.* 37, 1237–1247. <https://doi.org/10.1002/joc.5079>.
- Bano, I., Arshad, M., 2018. Climatic changes impact on water availability (chapter 2). In: Arshad, M. (Ed.), *Perspectives on Water Usage for Biofuels Production*. Springer, Cham. https://doi.org/10.1007/978-3-319-66408-8_2.
- Boluwade, A., 2020. Remote sensed-based rainfall estimations over the East and West Africa regions for disaster risk management. *ISPRS J. Photogrammetry Remote Sens.* 167C, 305–320. <https://doi.org/10.1016/j.isprsjprs.2020.07.015>.
- Boluwade, A., Stadnyk, T., Fortin, V., Roy, G., 2017. Assimilation of precipitation estimates from the integrated multisatellite Retrievals for GPM (IMERG, early run) in the Canadian precipitation analysis (CaPA). *J. Hydrol.: Reg. Stud.* 14, 10–22. <https://doi.org/10.1016/j.ejrh.2017.10.005>.
- Chen, F., Li, X., 2016. Evaluation of IMERG and TRMM 3B43 monthly precipitation products over mainland China. *Rem. Sens.* 8 (6), 472. <https://doi.org/10.3390/rs8060472>.
- Grimm, A.M., 2011. Interannual climate variability in South America: impacts on seasonal precipitation, extreme events, and possible effects of climate change. *Stoch. Environ. Res. Risk Assess.* 25 (4), 537–554. <https://doi.org/10.1007/s00477-010-0420-1>.
- Hou, A.Y., Kakar, R.K., Neeck, S., Azarbarzin, A.A., Kummerow, C.D., Kojima, M., Oki, R., Nakamura, K., Iguchi, T., 2014. The global precipitation measurement mission. *Bull. Am. Meteorol. Soc.* 95 (5), 701–722. <https://doi.org/10.1175/BAMS-D-13-00164.1>.
- Huang, W.R., Chang, Y.H., Liu, P.Y., 2018. Assessment of IMERG precipitation over Taiwan at multiple timescales. *Atmos. Res.* 214, 239–249. <https://doi.org/10.1016/j.atmosres.2018.08.004>.
- Nolasco, M.M., Ovando, G., Sayago, S., Magario, I., Bocco, M., 2021. Estimating soybean yield using time series of anomalies in vegetation indices from MODIS. *Int. J. Rem. Sens.* 42, 405–421. <https://doi.org/10.1080/01431161.2020.1809736>.
- Ovando, G., Sayago, S., Bellini Saibene, Y., Bocco, M., 2018. Evaluación del desempeño de productos satelitales para estimar precipitación en Córdoba (Argentina). In: *X Congreso de Agroinformática (CAI)-JAIIO 47*, vols. 3–7, pp. 203–214. Buenos Aires, September.
- Pérez, S., Sierra, E., Momo, F., Massobrio, M., 2015. Changes in average annual precipitation in Argentina's Pampa region and their possible causes. *Climate* 3 (1), 150–167. <https://doi.org/10.3390/cl3010150>.
- Prakash, S., Ramesh Kumar, M.R., Mathew, S., Venkatesan, R., 2017. How accurate are satellite estimates of precipitation over the North Indian Ocean? *Theor. Appl. Climatol.* 134 (1–2), 467–475. <https://doi.org/10.1007/s00704-017-2287-2>.
- Salles, L., Satgé, F., Roig, H., Almeida, T., Olivetti, D., Ferreira, W., 2019. Seasonal effect on spatial and temporal consistency of the new GPM-based IMERG-v5 and GSMAP-v7 satellite precipitation estimates in Brazil's central plateau region. *Water* 11 (4), 668. <https://doi.org/10.3390/w11040668>.
- Sun, W., Sun, Y., Li, X., Wang, T., Wang, Y., Qiu, Q., Deng, Z., 2018. Evaluation and correction of GPM IMERG precipitation products over the capital circle in northeast China at multiple spatiotemporal scales. *Adv. Meteorol.* 2018, 1–14. <https://doi.org/10.1155/2018/4714173>, 4714173.
- Sungmin, O., Foelsche, U., Kirchengast, G., Fuchsberger, J., Tan, J., Petersen, W.A., 2017. Evaluation of GPM IMERG Early, Late, and Final rainfall estimates using WegenerNet gauge data in southeastern Austria. *Hydrol. Earth Syst. Sci.* 21 (12), 6559–6572. <https://doi.org/10.5194/hess-21-6559-2017>.
- Tan, M.L., Santo, H., 2018. Comparison of GPM IMERG, TMPA 3B42 and PERSIANN-CDR satellite precipitation products over Malaysia. *Atmos. Res.* 202, 63–76. <https://doi.org/10.1016/j.atmosres.2017.11.006>.
- Tang, G., Zeng, Z., Long, D., Guo, X., Yong, B., Zhang, W., Hong, Y., 2016. Statistical and hydrological comparisons between TRMM and GPM level-3 products over a midlatitude basin: is day-1 IMERG a good successor for TMPA 3B42V7? *J. Hydrometeorol.* 17 (1), 121–137. <https://doi.org/10.1175/JHM-D-15-0059.1>.
- Taylor, K.E., 2001. Summarizing multiple aspects of model performance in a single diagram. *J. Geophys. Res.: Atmosphere* 106 (D7), 7183–7192. <https://doi.org/10.1029/2000JD900719>.
- Ulloa, J., Ballari, D., Campozano, L., Samaniego, E., 2017. Two-step down scaling of TRMM 3B43 V7 precipitation in contrasting climatic regions with sparse monitoring: the case of Ecuador in Tropical South America. *Rem. Sens.* 9 (7), 758. <https://doi.org/10.3390/rs9070758>.
- Verón, S.R., De Abelleira, D., Lobell, D.B., 2015. Impacts of precipitation and temperature on crop yields in the Pampas. *Climatic Change* 130 (2), 235–245. <https://doi.org/10.1007/s10584-015-1350-1>.
- Wang, X., Ding, Y., Zhao, C., Wang, J., 2019. Similarities and improvements of GPM IMERG upon TRMM 3B42 precipitation product under complex topographic and climatic conditions over Hexi region, Northeastern Tibetan Plateau. *Atmos. Res.* 218, 347–363. <https://doi.org/10.1016/j.atmosres.2018.12.011>.